

Comparison of calculated brightness and flux of radiation from a long-period wiggler and a short-period undulator

T. Shaftan,* S. L. Hulbert and L. Berman

National Synchrotron Light Source, Brookhaven National Laboratory, Upton, NY 11973, USA.

E-mail: shaftan@bnl.gov

In this article the calculation of brightness and flux for two insertion devices of the 2.8 GeV X-ray storage ring at the NSLS is discussed. The radiation properties from the X25 linearly polarized wiggler and the new X25 short-period undulator are compared at a fixed photon energy (11.3 keV) corresponding to emission from the fifth harmonic of the short-period undulator. For this computation, three commonly available synchrotron radiation programs are used. The capabilities of each of these codes are briefly discussed, and their range of applicability are commented on. It is concluded that special care is needed when modeling the radiation of the classes of insertion devices considered here.

© 2008 International Union of Crystallography

Printed in Singapore – all rights reserved

Keywords: flux; brightness; spectrum; undulator; wiggler.

1. Introduction

In the past, most experimental applications of synchrotron radiation were flux-limited, and in choosing a radiation source it was important to understand only the radiated flux from the source. More recently, the demands of experimental applications such as macromolecular crystallography and micro-diffraction have imposed rigid finesse requirements on the radiation beams they use, namely their opening angles, source dimensions and bandwidth. In these circumstances it becomes important to understand, when choosing a radiation source, not only the radiated flux but also the brightness of the source (Ablett *et al.*, 2004). Thus, it is crucial that calculations to distinguish the differences of flux and brightness of candidate radiation sources can be executed faithfully. As will be highlighted in this article, insertion device sources that might radiate comparable flux can have significantly different brightnesses. Although not a surprise, calculation codes which have sought to shed light on these properties of insertion devices have at times given inconsistent results.

We begin the paper by defining the problem, that includes three main parts: electron beam parameters, insertion device parameters, and geometric conditions for the radiation calculations. In the following we compare the flux and brightness of the considered insertion devices as calculated using three radiation codes [*URGENT (XOP)*, *SRW* and *SPECTRA*] with simple estimates and with each other.

2. Insertion devices, radiation sampling and electron beam

Table 1 summarizes the parameters of the linearly polarized wiggler (LPW) and short-period undulator (SPU). λ_u is the

period length, B_p is the peak magnetic field, and K is the magnetic strength parameter given by $K = 0.934B_p[T]\lambda_u[\text{cm}]$.

The parameters of the electron beam in the NSLS X-ray ring (J. Bengtsson, private communication) are summarized in Table 2. The values of the Twiss parameters in Table 2 correspond to a point at the center of a ring straight section. Horizontal-to-vertical coupling in the electron beam was taken to be 0.2%.

The goals of our computations were to determine the brightness, in units of photons s^{-1} (0.1% bandwidth) $^{-1} \text{mm}^{-2} \text{mrad}^{-2} \text{A}^{-1}$, and flux, in units of photons s^{-1} (0.1% bandwidth) $^{-1} \text{A}^{-1}$, for the LPW and SPU. A virtual horizontal aperture must be assumed at some distance from the insertion device (ID) in order to calculate the emitted flux in a way that facilitates useful comparison between wigglers and undulators. We chose a 10 mm-wide aperture located 10 m away from an

Table 1
Insertion device parameters.

	Number of poles	λ_u (cm)	B_p (T)	K
LPW	27	12	1.097	12.300
SPU	106	1.8	0.764	1.285

Table 2
Electron beam parameters.

Energy	$E = 2.8 \text{ GeV}$
Beam current	$I = 0.275 \text{ A}$
Horizontal emittance	$\epsilon_x = 60 \text{ nm}$
Vertical emittance	$\epsilon_y = 0.12 \text{ nm}$
Horizontal β -function	$\beta_x = 1.13 \text{ m}$
Horizontal dispersion	$\eta_x = 0.12 \text{ m}$
Vertical β -function	$\beta_y = 0.38 \text{ m}$
Energy spread	$\sigma_\gamma/\gamma = 0.1\%$

ID. This aperture corresponds to 1 mrad of horizontal angle and does not constrain the vertical divergence angle of radiation. Since the distance of 10 m substantially exceeds the length of both the LPW and the SPU, all computations were performed in the far-field approximation.

3. Synchrotron radiation programs

We have considered four synchrotron radiation codes for simulating the radiation output of the LPW and SPU. A short description of each code follows.

(i) *Synchrotron Radiation Workshop (SRW)*, version 4.0.6.1; Chubar & Elleaume, 1998) computes the synchrotron radiation from relativistic electrons in the near- and far-field range. It accepts a variety of input magnetic field profiles, including undulators, wigglers, bending magnets (central part and edges) and quadrupoles.¹ The polarization, spatial and angular intensity, and phase of the radiation, from millimeter wavelengths to the very hard X-ray range, are accurately computed for either a single electron or an electron beam with finite emittance and energy spread. For long wavelengths, CPU-efficient synchrotron radiation propagation is implemented using a Fourier optics approach that handles any number of drift spaces, diffracting apertures, lenses or focusing mirrors (Chubar & Elleaume, 1998).

(ii) *URGENT* (version 3.0; Walker & Diviacco, 1992) efficiently calculates the main properties of undulator radiation (spectral, angular, polarization and power density), including the effects of electron beam emittance and finite collection angles, for ideal plane, elliptical or helical trajectories, and also for the crossed-undulators scheme (Walker & Diviacco, 1992).

(iii) *SPECTRA* (version 6.1; Tanaka & Kitamura, 2001) can calculate properties of synchrotron radiation emitted from devices with a variety of magnetic field profiles, including undulators and wigglers of standard or exotic types, and bending magnets. For wigglers and bending magnets, the well known synchrotron radiation expressions are used. For undulator radiation, the so-called far-field approximation can be used for fast computation. For more accurate evaluation, expressions for synchrotron radiation emission in the near-field region are used for numerical computation. In this case, the properties of synchrotron radiation emitted from both ideal- and arbitrary-field devices can be calculated (Tanaka & Kitamura, 2001).

¹User comments: *SRW* estimates flux and brightness based on the analytic formulas. Numerical calculation is provided in units of flux [photons s⁻¹ (0.1% bandwidth)⁻¹] or flux per unit area [photons s⁻¹ (0.1% bandwidth)⁻¹ mm⁻²] for an undulator. For a wiggler, *SRW* numerically calculates the flux per unit area [photons s⁻¹ (0.1% bandwidth)⁻¹ mm⁻²]. Emittance and energy spread are fully included into numerical calculations.

URGENT calculates radiation parameters fully including beam emittance and energy spread. *URGENT* calculates flux and brightness for an undulator, but only flux for a wiggler. *URGENT* crashes when the number of undulator periods exceeds several hundred. *URGENT* gives an error in the flux calculation: it scales the result linearly with aperture area. It takes into account the electron beam size in the middle of the undulator or wiggler.

SPECTRA calculates flux and brightness for an undulator and wiggler taking into account emittance and energy spread of the electron beam. Calculation of radiation parameters does not proceed correctly for wigglers with magnetic strength parameter $K > 10$.

(iv) *XOP (X-ray Oriented Programs)*, version 2.1; Sánchez del Río & Dejus, 1998) is a widget-based driver program that is used as a common front-end interface for computer codes of interest to the synchrotron radiation community. It provides codes for modeling of X-ray sources (e.g. synchrotron radiation sources, such as undulators and wigglers), characteristics of optical devices (mirror, filters, crystals, multilayers etc.) and multipurpose data visualizations and analyses (Sánchez del Río & Dejus, 1998). *XOP* contains a very broad range of applications for calculation of various radiation properties and propagating them to the user endstation. *XOP* uses *URGENT* (see above) to calculate the flux and brightness of wiggler and undulator sources. Therefore, we will refer to *XOP* and *URGENT* as *URGENT/XOP* throughout this article.

4. Electron beam and photon output properties for LPW and SPU

Below we provide a list of estimates of various electron beam and radiation output parameters for LPW and SPU (Murphy, 2001, and references therein).

Electron beam horizontal size at the center of an ID (RMS):

$$\sigma_x = [\beta_x \varepsilon_x + (\eta_x \delta)^2]^{1/2} = 0.287 \text{ mm.} \quad (1)$$

Electron beam vertical size at the center of an ID (RMS):

$$\sigma_y = (\beta_y \varepsilon_y)^{1/2} = 0.0068 \text{ mm.} \quad (2)$$

Electron beam horizontal divergence angle (RMS):

$$\sigma'_x = (\varepsilon_x / \beta_x)^{1/2} = 0.2304 \text{ mrad.} \quad (3)$$

Electron beam vertical divergence angle (RMS):

$$\sigma'_y = (\varepsilon_y / \beta_y)^{1/2} = 0.0178 \text{ mrad.} \quad (4)$$

SPU first-harmonic photon wavelength and energy (*SRW*: 2.230 keV):

$$\lambda_1 = \frac{\lambda_u}{2\gamma^2} (1 + K^2/2) = 5.472 \text{ \AA} \quad \text{and} \\ h\nu_1 = 12.398/\lambda_1 [\text{A}] = 2.266 \text{ keV.} \quad (5)$$

SPU fifth-harmonic photon wavelength and energy (*SRW*: 11.300 keV):

$$\lambda_5 = \frac{\lambda_u}{10\gamma^2} (1 + K^2/2) = 1.094 \text{ \AA} \quad \text{and} \\ h\nu_5 = 12.398/\lambda_5 [\text{A}] = 11.327 \text{ keV.} \quad (6)$$

LPW critical photon energy:

$$h\nu_{\text{cr}} = 712.019 K E^2 [\text{GeV}]/\lambda_u [\text{cm}] = 5.722 \text{ keV.} \quad (7)$$

SPU first-harmonic radiation beam divergence angle (RMS):

$$\sigma'_{r1} = (\lambda_1 / L_{\text{SPU}})^{1/2} = 0.0240 \text{ mrad.} \quad (8)$$

SPU fifth-harmonic radiation beam divergence angle (RMS):

$$\sigma'_{r5} = (\lambda_5 / L_{\text{SPU}})^{1/2} = 0.0107 \text{ mrad.} \quad (9)$$

LPW horizontal beam divergence angle (at the critical energy, RMS):

$$\sigma'_{cr,x} = K/2\gamma = 1.122 \text{ mrad.} \quad (10)$$

LPW vertical beam divergence angle (at the critical energy, RMS):

$$\sigma'_{cr,y} = 1/\gamma = 0.182 \text{ mrad.} \quad (11)$$

LPW vertical beam divergence angle (at 11.3 keV, RMS; Hulbert & Weber, 1992):

$$\sigma_\psi = \left(\frac{2\pi}{3}\right)^{1/2} \frac{1}{\gamma Y} \frac{\int_Y^\infty K_{5/3}(x) dx}{K_{2/3}^2(Y/2)} = 82.0 \mu\text{rad.} \quad (12)$$

SPU first-harmonic spectral width (RMS):

$$\Delta\lambda_1/\lambda_1 = 1/N = 1.920\%. \quad (13)$$

SPU fifth-harmonic spectral width (RMS):

$$\Delta\lambda_5/\lambda_5 = 1/(5N) = 0.377\%. \quad (14)$$

Broadening of SPU harmonics owing to the horizontal divergence of the electron beam (RMS):

$$\Delta\lambda/\lambda = (\gamma\sigma'_x)^2/(1 + K^2/2) = 0.873\%. \quad (15)$$

Broadening of SPU harmonics owing to the energy spread of the electron beam (RMS):

$$\Delta\lambda/\lambda = 2\delta \simeq 0.2\%. \quad (16)$$

Broadening of SPU harmonics owing to the horizontal acceptance half angle ($\theta = 0.5$ mrad):

$$\Delta\lambda/\lambda = (\gamma\theta)^2/(1 + K^2/2) = 4.111\%. \quad (17)$$

LPW flux per 1 mrad of horizontal angle at 11.3 keV:

$$\begin{aligned} F_{LPW} &= 2.458 \times 10^{13} 2NE[\text{GeV}] Y \int_Y^\infty K_{5/3}(\eta) d\eta \\ &= 5.72 \times 10^{14} \text{ photons s}^{-1} (0.1\% \text{ bandwidth})^{-1} \\ &\quad \text{mrad}^{-1} \text{ A}^{-1}. \end{aligned} \quad (18)$$

SPU brightness (central cone) at first and fifth harmonics (SRW estimate; Murphy, 2001, and references therein):

$$\begin{aligned} E_{SPU,1} &= 9.604 \times 10^{18} \text{ photons s}^{-1} (0.1\% \text{ bandwidth})^{-1} \\ &\quad \text{mm}^{-2} \text{ mrad}^{-2} \text{ A}^{-1}, \\ E_{SPU,5} &= 1.244 \times 10^{18} \text{ photons s}^{-1} (0.1\% \text{ bandwidth})^{-1} \\ &\quad \text{mm}^{-2} \text{ mrad}^{-2} \text{ A}^{-1}. \end{aligned} \quad (19)$$

Here, subscripts x and y correspond to the horizontal and vertical planes, respectively, ε , γ and δ are the electron beam emittance, energy (in units of electron rest mass; E is the value in GeV) and energy spread, respectively, β and η are the electron beam β function and dispersion at the center of the insertion device, respectively, λ_u and K are the undulator period length and magnetic strength parameter, respectively, $h\nu$ is the photon energy, and $Y = h\nu/h\nu_{cr}$.

5. Calculations of transverse spot properties

For the calculation of transverse spot properties we used the *SRW* program. The electron beam and radiation sampling parameters are given in Tables 1 and 2. Fig. 1 shows the LPW flux distribution 10 m away from the wiggler. The flux is calculated for 0.1% energy bandwidth at a fixed photon energy of 11.3 keV. The resulting RMS spot sizes are 12.1 mm horizontally and 0.86 mm vertically. Assuming that the electron beam source size is small compared with these values (a rather good assumption, see §4 above), these spot sizes correspond to RMS divergence angles of 1.21 mrad horizontally and 0.086 mrad vertically.

Fig. 2 shows the SPU flux distribution 10 m away from the center of the undulator, calculated at a fixed photon energy of 11.3 keV (fifth harmonic) in a 0.1% bandwidth. The calculated RMS sizes (angles) are 2.3 mm (0.23 mrad) horizontally and 0.21 mm (0.021 mrad) vertically.

6. Spectra of radiation for realistic and filament electron beams

Fig. 3 presents the LPW spectral flux per unit area for the cases of a realistic electron beam (with emittance, with energy spread, blue) and filament electron beam (no emittance, no energy spread, red).

Fig. 4 shows SPU flux spectra for the cases of a realistic electron beam (with emittance, with energy spread, blue) and

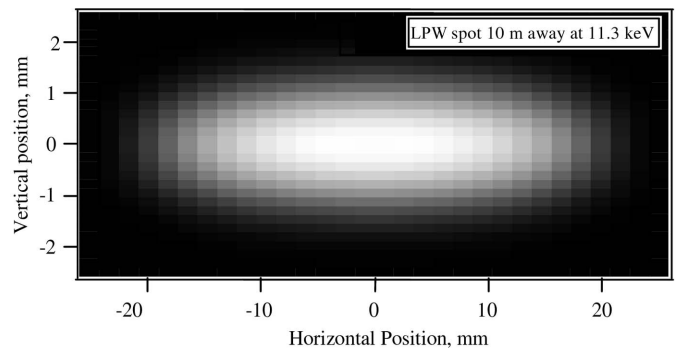


Figure 1 LPW transverse flux distribution at 10 m from the center of the wiggler at 11.3 keV photon energy.

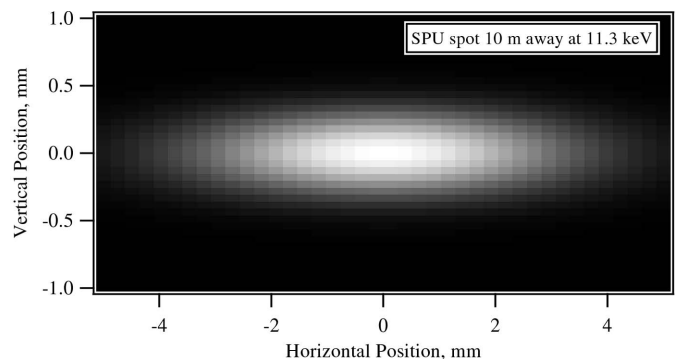


Figure 2 SPU transverse flux distribution at 10 m from the center of the undulator at 11.3 keV photon energy.

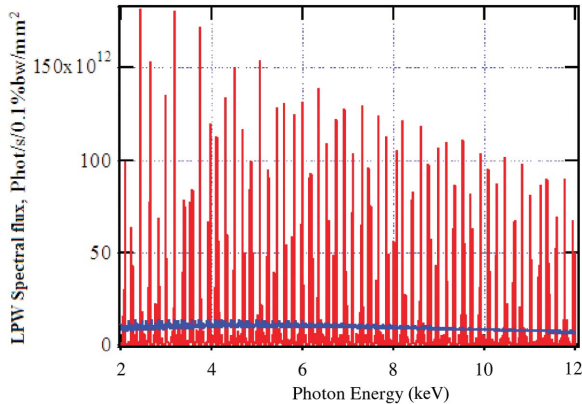


Figure 3 LPW flux density spectra for the cases of realistic (blue curve) and filament (red curve) electron beam parameters calculated by *SRW*.

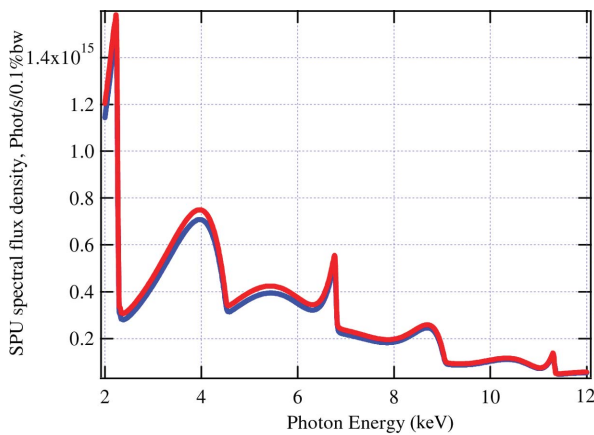


Figure 4 SPU flux density spectra for the cases of realistic (blue curve) and filament (red curve) electron beam parameters calculated by *SRW*.

filament electron beam (no emittance, no energy spread, red). We conclude that the flux spectra are almost independent of electron beam parameters because they are proportional to the total number of photons emitted. However, the flux per unit area and brightness are strongly dominated by the realistic electron beam parameters.

7. Brightness

Fig. 5 shows the brightness of the LPW. The red curve on the left plot is given by the *URGENT/XOP* calculation. The dense harmonics of the strong ($K \approx 10$) wiggler create the fuzzy structure in the calculated brightness spectrum. The black curve is generated by the analytic estimate in *SRW*. Both *SPECTRA* and *SRW* use only an analytic estimate to estimate wiggler brightness.

The figure in the right-hand plot of Fig. 5 is an expanded region of the brightness spectra in the neighborhood of 11.3 keV. The 8 eV energy separation

between peaks corresponds to the first-harmonic frequency of the LPW.

Calculating the LPW brightness using analytic formula (Hulbert & Weber, 1992) gives the following value at 11.3 keV,

$$B_{\text{LPW}} = 2.1 \times 10^{17} \text{ photons s}^{-1} (0.1\% \text{ bandwidth})^{-1} \text{ mm}^{-2} \text{ mrad}^{-2} \text{ A}^{-1}.$$

Fig. 6 shows the brightness of the SPU (left) and the expanded region near the fifth harmonic at 11.3 keV (right). The brightness calculated using *URGENT/XOP* (red) agrees well with that using *SPECTRA* (blue). The black curves in Fig. 6 are produced by the brightness estimate in *SRW* that is based on an analytical formula [Murphy, 2001, see equation (19), §3].

8. Flux

For assessing the LPW flux calculation we used the following method. *SRW* can calculate the flux per unit area for an arbitrary wiggler. Fig. 7 shows the horizontal and vertical flux densities produced by *SRW* at a photon energy of 11.3 keV in a bandwidth of 0.1%, which can be compared with the LPW spot figure in §5 above.

The areas under the curves in Fig. 7 were evaluated by numerical integration, yielding an LPW flux at 11.3 keV for 1 mrad horizontal angular extent (the range shown in Fig. 7 left) of

$$F_{\text{LPW}} = 4.62 \times 10^{14} \text{ photons s}^{-1} (0.1\% \text{ bandwidth})^{-1} \text{ mrad}^{-1} \text{ A}^{-1}.$$

SRW estimates the value of the LPW flux per mrad of the horizontal angle as

$$F_{\text{LPW}} = 6.68 \times 10^{14} \text{ photons s}^{-1} (0.1\% \text{ bandwidth})^{-1} \text{ mrad}^{-1} \text{ A}^{-1}.$$

We also used an estimate, based on representing wiggler flux as the flux of equivalent dipole sources multiplied by the number of wiggler poles ($2N$ formula'),

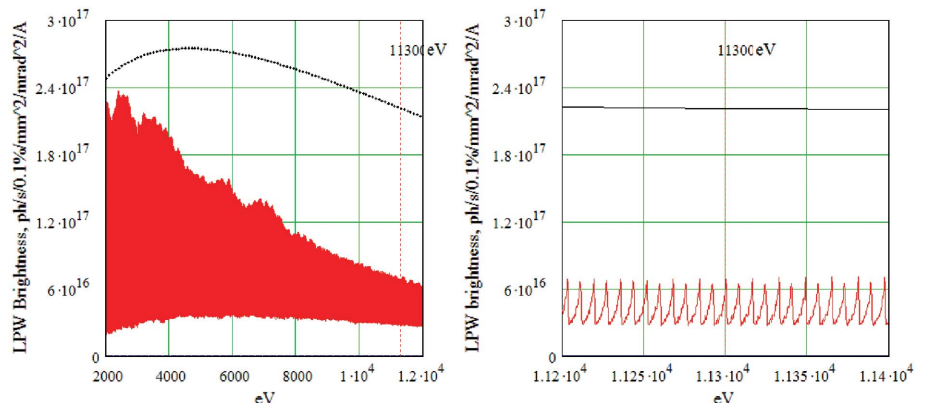


Figure 5 Calculated brightness of the LPW from *URGENT* (red curves) and *SPECTRA* (blue curves) calculations. Wide range spectra (left) and close-up near 11.3 keV (right).

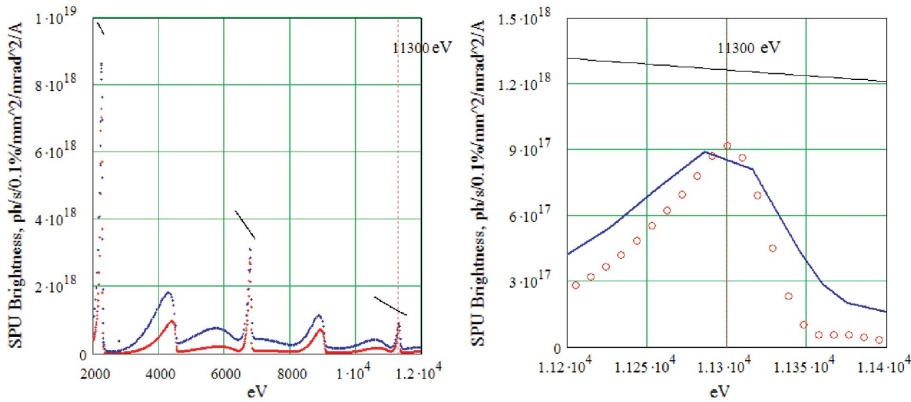


Figure 6
Calculated brightness of the SPU from *URGENT* (red points) and *SPECTRA* (blue points) calculations. Wide range spectra (left) and close-up near 11.3 keV (right).

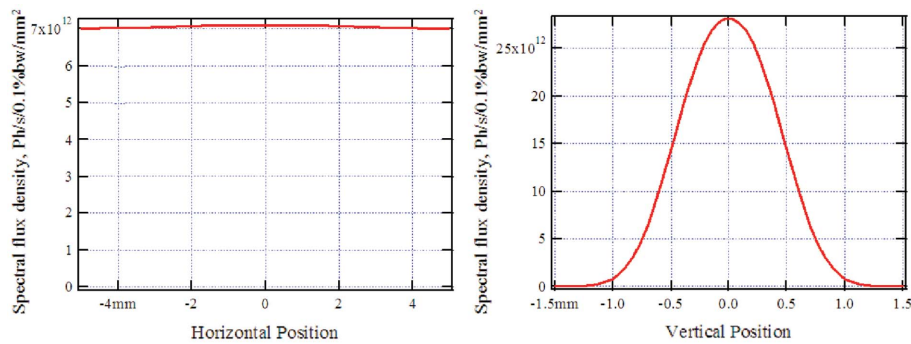


Figure 7
LPW flux density at 11.3 keV photon energy on a normal-incidence surface located 10 m from the source.

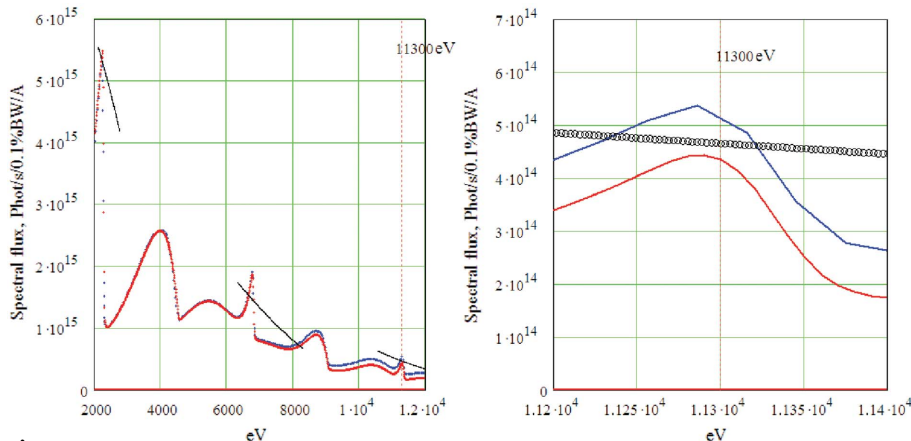


Figure 8
Calculated flux of SPU, from *SRW* (red) and *SPECTRA* (blue). Wide range spectra (left) and close-up near 11.3 keV (right).

$$F_{\text{LPW}} = 5.72 \times 10^{14} \text{ photons s}^{-1} (0.1\% \text{ bandwidth})^{-1} \text{ mrad}^{-1} \text{ A}^{-1}.$$

Fig. 8 shows the values of the SPU flux determined by *SPECTRA* (blue) and *SRW* (red). The third set of curves (in black on the right-hand plot, and circles on the left-hand) is the *SRW* estimate. The flux values at 11.3 keV (fifth harmonic) calculated by the different programs are in good agreement with each other.

9. Comparison with estimates

The exact harmonic photon energies in all codes slightly differ from the values given by equations (5) and (6) in §4 above. A particular explanation for this discrepancy lies in the dependence of the photon energy for a given harmonic on the number of undulator periods (Coisson & Tatchyn, 1985) illustrated in Fig. 9.

In Fig. 10 we plot the dependence of the detuning ratio and relative intensity gain for the first harmonic of the SPU as a function of the number of periods. The vertical red dashed lines on these plots indicate the number of periods in the NSLS SPU, so that the intersecting horizontal red dashed lines read out the detuning ratio and intensity loss. The blue dashed line in the detuning ratio plot corresponds to an estimate of the detuning given by $\Delta f_n/f_n \simeq 1 - 1/(nN)$.

Fig. 10 indicates that the SPU detuning ratio should be about 0.985. The value calculated by *SRW* is 0.9842. The intensity loss for the first harmonic is 10%. For the fifth harmonic the detuning ratio is calculated to be 0.9976.

With horizontal divergence angles given by equations (3) and (9) in §4, the RMS horizontal spot size of the SPU fifth harmonic is estimated to be 2.3 mm at 10 m downstream of the undulator source point. Using vertical divergence angles given by equations (4) and (9) in §4, we arrive at a vertical spot size for the SPU fifth harmonic of 0.21 mm (RMS, 10 m downstream of the undulator). These values are in good agreement with the value calculated using *SRW* (see §5).

Using the vertical divergence angle given by equation (12) in §4, we obtain a vertical spot size for the LPW radiation at 11.3 keV of 0.82 mm (RMS, 10 m downstream of the undulator). This value is in good agreement with the value calculated using *SRW* (see §5). The horizontal spot size (11.2 mm) is estimated using equation (10) of §4 and is in agreement with the value obtained at the LPW critical energy.

10. Comparison

In this section we compare the LPW and SPU brightness and flux values obtained by numerical simulations undertaken in this work with estimates obtained from analytic formulae.

Brightness in units of photons s^{-1} (0.1% bandwidth) $^{-1}$ mm $^{-2}$ mrad $^{-2}$ A $^{-1}$ is provided in Table 3, while flux in units of photons s^{-1} (0.1% bandwidth) $^{-1}$ A $^{-1}$ is given in Table 4.

From Tables 3 and 4, we conclude that the agreement between our calculations and estimates is good. However, there is an obvious disagreement (a factor of about five) between the LPW brightness value calculated using *URGENT/XOP* and the estimated value from *SRW*.

We also note that the X25 upgrade, from LPW to SPU, did not increase the amount of radiated flux, but increased the X25 brightness by a factor of five according to Table 3.

11. Conclusions

A sensible comparison of the benefits of wigglers *versus* undulators for various synchrotron radiation applications, such as the macromolecular crystallography application at NSLS beamline X25, depends crucially on the efficacy of computation codes to calculate faithfully the flux and brightness of these radiation sources. The ability to compare these two types of sources properly is even more important for synchrotron sources whose emittances are not state-of-the-art than for those whose emittances are.

We would like to thank J. B. Murphy for initiating this work and for many important discussions and corrections. The manuscript has been authored by Brookhaven Science Associates, LLC under Contract No. DE-AC02-98CH10886 with the US Department of Energy. The United States Government retains, and the publisher, by accepting the

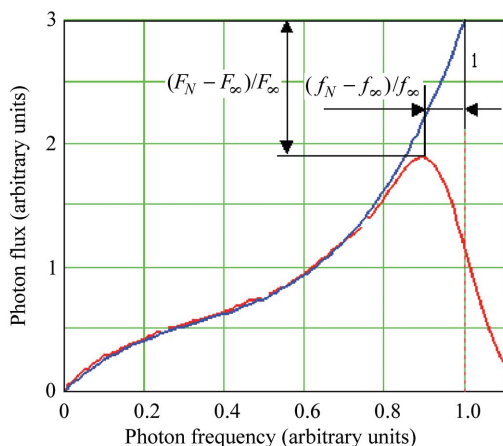


Figure 9 Normalized spectra of the first harmonic for the undulators with $N = 10$ (red curve) and $N = 1000$ (∞ , blue curve) periods. The quantities indicated correspond to the peak intensity detuning and reduction in photon frequency owing to the finite number of undulator periods.

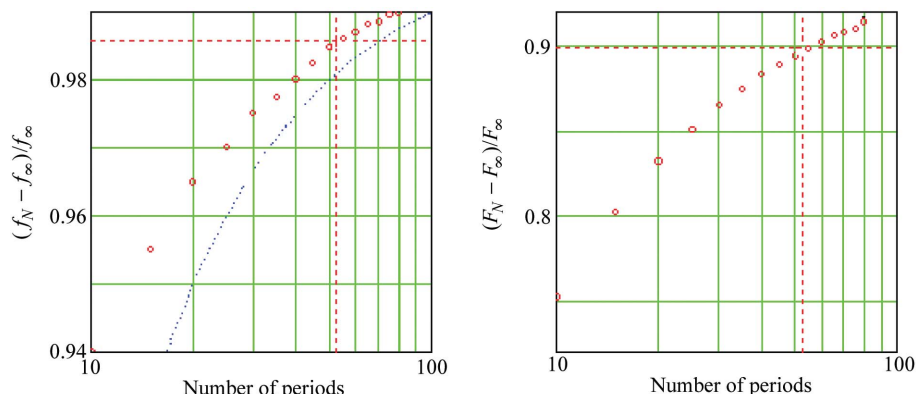


Figure 10 Dependence of undulator first-harmonic detuning ratio (left) and first-harmonic intensity gain (right) on the number of undulator periods. Red dashed lines correspond to the specific values for the NSLS SPU.

Table 3

Comparison of calculated brightness values.

Units of brightness: photons s^{-1} (0.1% bandwidth) $^{-1}$ mm $^{-2}$ mrad $^{-2}$ A $^{-1}$.

	SRW estimate	Calculation
LPW	2.2×10^{17}	0.52×10^{17} (<i>URGENT/XOP</i>)
SPU	1.2×10^{18}	9×10^{17} (<i>SPECTRA</i> , <i>URGENT/XOP</i>)

Table 4

Comparison of calculated flux values.

Units of flux: photons s^{-1} (0.1% bandwidth) $^{-1}$ A $^{-1}$.

	SRW estimate	Calculation
LPW	6.7×10^{14}	4.6×10^{14} (<i>SRW</i>), 5.72×10^{14} ('2N' formula)
SPU	4.7×10^{14}	5.1×10^{14} (<i>SPECTRA</i>), 4.4×10^{14} (<i>SRW</i>)

article for publication, acknowledges, a worldwide license to publish or reproduce the published form of this manuscript, or allow others to do so, for the United States Government purposes.

References

Ablett, J. M., Berman, L. E., Kao, C. C., Rakowsky, G. & Lynch, D. (2004). *J. Synchrotron Rad.* **11**, 129–131.
 Chubar, O. & Elleaume, P. (1998). *Proceedings of the Sixth European Particle Accelerator Conference (EPAC98)*, 22–26 June 1998, Stockholm, Sweden, p. 1177.
 Coisson, R. & Tatchyn, R. (1985). *International Conference on Insertion Devices for Synchrotron Sources*, 27–30 October 1985, Stanford, CA, USA, p. C-45.
 Hulbert, S. L. & Weber, J. M. (1992). *Nucl. Instrum. Methods*, **A319**, 25–31.
 Murphy, J. B. (2001). *Synchrotron Light Source Data Book*, BNL report 42333 rev., edited by A. Thompson *et al.*, *X-ray Data Booklet*, LBNL/PUB-490, rev. 2.
 Sánchez del Río, M. & Dejus, R. J. (1998). *Proc. SPIE*, **3448**, 340–345.
 Tanaka, T. & Kitamura, H. (2001). *J. Synchrotron Rad.* **8**, 1221–1228.
 Walker, R. P. & Diviacco, B. (1992). *Rev. Sci. Instrum.* **63**, 392–395 (see also Sincrotrone Trieste report ST/M-91/12).